Direct Surface Structure Determination with Photoelectron Diffraction

J. J. Barton, C. C. Bahr, Z. Hussain,[a] S. W. Robey, J. G. Tobin, L. E. Klebanoff, and D. A. Shirley
Materials and Molecular Research Division, Lawrence Berkeley Laboratory, Berkeley, California 94720, and Departments of Chemistry and Physics, University of California, Berkeley, California 94720

(Received 3 February 1983)

Angle-resolved photoemission extended fine structure from adsorbate core levels yields complete, accurate surface structures without resort to trial-and-error comparisons to theory. Scattering peaks from individual substrate atoms were observed with use of S(1s) photoemission from $c(2\times2)$S/Ni(001) and $p(2\times2)$S/Cu(001), along [011]. Fourfold-hollow site geometries were found for both systems, with interatomic distances of R(S-Ni) $=2.24(3)$ Å and R(S-Cu) $=2.28(3)$ Å.

PACS numbers: 68.20.+t, 61.14.-x

In this Letter we show that photoelectron diffraction data, in the form of angle-resolved photoemission extended fine structure (ARPEFS) from adsorbate core levels, can be transformed to give path-length differences between primary and substrate-atom-scattered photoelectron waves. Analysis of these path-length differences yields *both* distances and directions to nearby substrate atoms. For a given system, ARPEFS curves for one or more directions will thus provide a complete surface structure determination.

Energy-dependent photoelectron diffraction[1,2] has been used to determine adsorbate-substrate geometries for a number of systems.[3] Experimentally, photoemission into a selected angle is measured while the photoelectron kinetic energy is swept by varying a tunable photon source. Until now, analysis of the intesntiy variations with energy has been limited to trial-and-error comparisons with the results of scattering calculations.[4] Recently, normal-emission theoretical curves over extended energy ranges,[5] and experimental curves over short ranges,[6] were Fourier analyzed to yield peaks at distances close to adsorbate-substrate interplanar spacings, but the role of scattering phase shifts and the utility of this approach remained unclear.

Direct analysis begins by deriving the ARPEFS curve from the photoemission measurements. As shown in Fig. 2(a), the intensity modulations, $\chi(E)$, are extracted by removing the smooth atomic cross section: $\chi(E)=(I-I_0)/I_0$, where I is the measured intensity and I_0 is the atomic partial cross section.[7] Then the de Broglie relation is used to convert from electron kinetic energy to electron wave vector, $k=[2m(E-E_0)/\hbar^2]^{1/2}$, where E_0 is adjusted empirically to minimize the difference between theoretical and experimental scattering phase shifts,[14] as is done in the analysis of EXAFS data. In fact, the ARPEFS E_0 is similar, but not identical, to the EXAFS E_0, as discussed below. A single-scattering model[8] for photoelectron diffraction predicts the resulting ARPEFS modulations according to

$$\chi(k)=\sum_j \frac{\cos\beta_j}{\cos\gamma}\frac{|f(\alpha_j)|}{r_j} \times\cos[kr_j(1-\cos\alpha_j)+\varphi_j], \quad (1)$$

where the photoelectron wave encounters an ion core at a distance r_j from the source atom, scatters through an angle α_j with amplitude $|f(\alpha_j)|$, and, after a phase shift φ_j, propagates towards the detector. The angle between the polarization direction and the direct emission path is γ; the angle between the polarization direction and the initial path of an electron scattered from site j is β_j. Figure 1 illustrates the scattering geom-

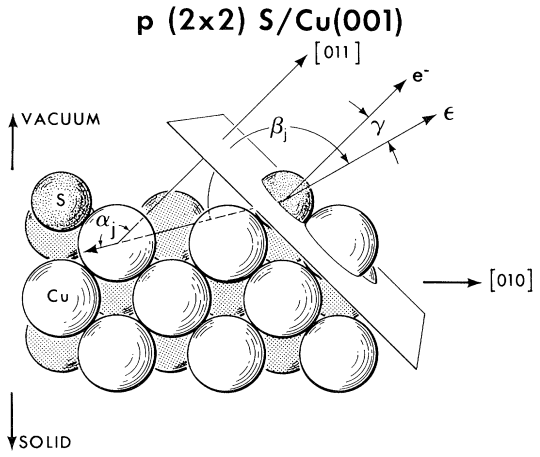

FIG. 1. Cross-sectional view of a fcc crystal (001) surface showing the experimental geometry and illustrating the parameters of the analytic single-scattering formula. The angle-resolved detector is along the vector labeled e^- ([011] direction); the polarization vector is ϵ. The angle between these two vectors is γ. The vector from the emitter to the scattering atom j makes an angle β_j with the polarization vector and an angle α_j with the emission direction.

etry.

Equation (1) suggests that a rather large number of path-length differences $\Delta R_j = r_j(1-\cos\alpha_j)$ can contribute to $\chi(k)$. However, two factors combine to emphasize the contributions from scatterers lying more or less directly behind the source atom (i.e., α_j near 180°). First, as Orders and Fadley[9] noted, $f(\alpha_j)$ tends to peak strongly near $\alpha_j = 0°$ and 180°, for electrons in the ARPEFS energy range of 100–400 eV. Second, the factor $\cos\beta_j/\cos\gamma$ in Eq. (1) suppresses scattering from atoms at angles near 90° when the polarization direction is pointed into the detector.

The strong peaking in scattering amplitude near $\alpha_j = 180°$ suggests that alignment of the detector, an adsorbate atom, and a substrate atom along the polarization direction would yield large ARPEFS modulations with a frequency near $2r_j$, i.e., twice the bond distance. Figure 2 shows the results of two such experiments for S(1s) photoemission along [011] in the overlayer systems $c(2\times2)$S/Ni(001) and $p(2\times2)$S/Cu(001), which were prepared by standard techniques.[6,10] Figures 2(a) and 2(b) both show large oscillations, and both contain the same dominant frequency. Since several reports[6,11] agree that S bonds in the fourfold-hollow site on Ni(001), we may immediately conclude that S bonds in this same site on Cu(001). The energy range spanned by the S/Ni curve corresponds to a wave-number range in reciprocal angstroms of approximately one period (2π); the presence of four major oscillations thus indicates a path-length difference ΔR of ~4 Å.

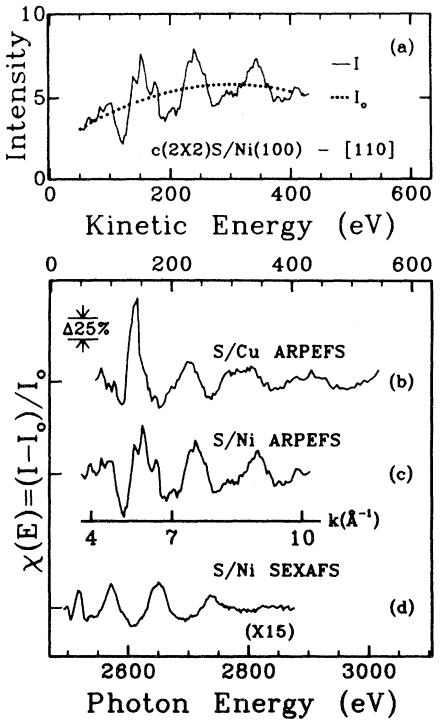

FIG. 2. (a) Photoemission partial-cross-section measurements for $c(2\times2)$S/Ni(100). The curve I represents the area of the elastic photopeak, divided by the background emission to correct for photon flux, multiplied by kinetic energy to correct for electron-analyzer transmission, and divided by 100 000. The curve I_0 is described in Ref. 7. $\chi(E)$ curves are shown for (b) $p(2\times2)$S/Cu(001) ARPEFS in the [011] direction with $\gamma = 15°$, (c) $c(2\times2)$S/Ni(001) ARPEFS in the [011] direction with $\gamma = 0°$, and (d) $c(2\times2)$S/Ni(001) SEXAFS from Brennan, Stohr, and Jaeger (Ref. 11).

The ARPEFS data in Fig. 2 were analyzed by an autoregressive linear prediction procedure,[12] followed by Fourier analysis, yielding the curves shown in Fig. 3. The excellent resolution is a consequence of the autoregression step. *The first three peaks in the middle curve of Fig. 3 at ΔR values of 2.0, 3.5 and 4.4 Å, all arise from the four nearest-neighbor nickel atoms along [110], lying respectively in front of, beside (two Ni atoms), and almost directly behind the sulfur atom.* The general form of these peaks establishes without further analysis that sulfur lies in a fourfold-hollow site 1.3–1.4 Å above the surface, in agreement with the known structure.[6,11] This curve alone approaches being a complete self-contained structure determination, because these three peaks carry information about interatomic distances and directions to each nearest-neighbor

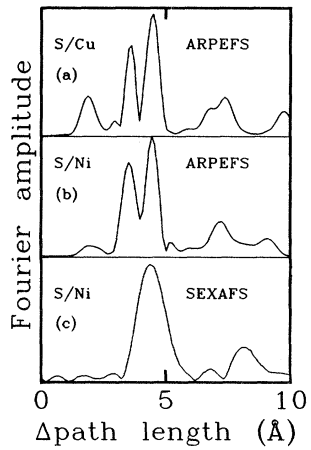

FIG. 3. Comparison of Fourier-transform amplitudes for (a) ARPEFS from $p(2\times2)$S/Cu(001), (b) ARPEFS from $c(2\times2)$S/Ni(001), and (c) SEXAFS from $c(2\times2)$S/Ni(001) from Ref. 11. The ARPEFS range in k space was extended with use of the autoregressive estimation method prior to Fourier transformation.

Ni atom separately. Because the scattering phase shifts are known[13] most reliably for 180° backscattering, full analysis for path-length difference was applied to the $\Delta R = 4.42$-Å peak alone. Following Martens *et al.*,[14] the Fourier peak was back transformed, the theoretical phase shift was subtracted from the total phase, and the result was divided by k to give a path-length difference curve. The empirical E_0 was adjusted to give a constant path-length difference from $k = 5$ to $k = 10$ Å^{-1}. We derive R(S-Ni) = 2.24(3) Å, in excellent agreement with the result of Brennan, Stohr, and Jaeger.[11]

A similar analysis on the "unknown" system $p(2\times 2)$Cu(001) yields similar results: a fourfold-hollow site with $\Delta R = 4.54$ Å, and R(S-Cu) = 2.28(3) Å [Figs. 2(b) and 3(a)]. The structure of $p(2\times 2)$ S/Cu(001) is thus determined.

The ARPEFS curves for both S/Ni and S/Cu show peaks for path lengths greater than 5 Å. These features correspond to second- and third-nearest-neighbor scattering atoms, but they are not individually resolved and will require detailed comparison to scattering calculations for evaluation.

Comparing the S/Ni and S/Cu Fourier transforms reveals another important ARPEFS feature: The intensities of peaks corresponding to atoms with $\beta_j \sim 90°$ will be strongly dependent on the polarization direction. The S/Ni measurements were made with the polarization vector aligned along the emission vector. The nearest neighbor with the shortest path length has $\cos\beta_j/\cos\gamma = 0.12$. For S/Cu we tipped the polarization vector 15° closer to the surface, increasing the photoemission flux onto this atom—and hence the size of the first peak—by a factor of 5: $\cos\beta_j/\cos\gamma = 0.63$. This polarization dependence provides a sensitive means for determining the exact angular position of individual substrate atoms.

Our results also provide a useful comparison of the ARPEFS and surface extended x-ray–absorption fine-structure (SEXAFS) techniques.[15] Figures 2(d) and 3(c) reproduce the SEXAFS modulations and Fourier transform reported by Brennan, Stohr, and Jaeger.[11] SEXAFS is an angle-integrated measurement of the absorption cross section. Its modulations vary as $\sin(2kr + \varphi_b + \varphi_a)$, oscillating with a frequency close to twice the bond length. ARPEFS is an angle-resolved measurement following $\cos[kr_j(1 - \cos\alpha_j) + \varphi_j]$. The frequency evident in Figs. 2(b) and 2(c) is close to twice the bond length because the modulations are dominated by scattering from the nearest neighbor directly behind the sulfur. SEXAFS has both an absorber and a backscatterer phase shift; ARPEFS has only a backscatterer shift. The SEXAFS modulations are ±2%; the ARPEFS modulations are larger by $kr_j \sim 10$. The SEXAFS polarization dependence has the form of an intensity $(\cos^2\beta_j)$; the ARPEFS polarization dependence follows an amplitude $(\cos\beta_j)$. But Fig. 3 illustrates the most important difference: Each near neighbor appears as a separate peak in the ARPEFS Fourier transform. The positions and intensities of these peaks carry information about the distances *and* directions of neighboring atoms and they can be varied by adjusting the emission and polarization vectors.

Finally, we note that a physically significant E_0 may be derivable for ARPEFS. As recently discussed by Bunker and Stern,[16] the EXAFS E_0 is sensitive to the charge state of the photoabsorber, to the intensity of photoemission satellite features, to selection of the absorption-edge reference, and to the breakdown in the small-atom approximation. Since photoemission measures the scattered photoelectron's kinetic energy, only the inner potential of the solid and the small-atom approximation should determine E_0. The simple single-scattering nature of ARPEFS suggests that a theoretical calculation of the scattering phase should be possible, allowing comparison of E_0 to a known inner potential.

In summary, we have reported experimental evidence for the dominance of single backscattering in photoelectron diffraction. The use of ARPEFS directly to solve the $p(2\times 2)$S/Cu(001) structure demonstrates its power as a probe for surface structures. With the increasing performance of synchrotron radiation facilities, wide energy-range photoemission data can be obtained for all elements, including the technologically and biologically important low-Z elements. The angle-resolved nature of ARPEFS gives its promise for the study of molecular and multisite atomic adsorbates. Disputed surface structures may be determined unambiguously by placing an angle-resolved detector opposite an expected substrate atom and recording the resultant ARPEFS. Complicated adsorbate systems can be analyzed along a variety of emission axes. By careful choices and variation of emission and polarization directions, it may even be feasible to determine bond angles to within 1–2°.

We thank P. Orders and C. Fadley for helpful discussions and the use of their partial-wave phase shifts.

This work was supported by the Director, Office of Energy Research, Office of Basic Energy Sciences, Chemical Sciences Division of the U.S. Department of Energy under Contract No. DE-AC03-76SF00098. It was performed at the Stanford Synchrotron Radiation Laboratory, which is supported by the National Science Foundation through the Division of Materials Research. We also acknowledge support from the University of Petroleum and Minerals and the National Science Foundation.

---

[a]Present address: University of Petroleum and Minerals, Dhahran, Saudi Arabia.

[1]A. Liebsch, Phys. Rev. Lett. 32, 1203 (1974).

[2]S. D. Kevan, D. H. Rosenblatt, D. R. Denley, B.-C. Lu, and D. A. Shirley, Phys. Rev. Lett. 41, 1565 (1978).

[3]S. Y. Tong and C. H. Li, Crit. Rev. Solid State Sci. 10, 209 (1981).

[4]S. Y. Tong, C. H. Li, and A. R. Lubinsky, Phys. Rev. Lett. 39, 498 (1977); C. H. Li, A. R. Lubinsky, and S. Y. Tong, Phys. Rev. B 17, 3128 (1978).

[5]Z. Hussain, D. A. Shirley, C. H. Li, and S. Y. Tong, Proc. Nat. Acad. Sci. U.S.A. 78, 5293 (1981).

[6]D. H. Rosenblatt, J. G. Tobin, M. G. Mason, R. F. Davis, S. D. Kevan, D. A. Shirley, C. H. Li, and S. Y. Tong, Phys. Rev. B 23, 3828 (1981).

[7]The exact form chosen for I_0 has little effect on the structural analysis. Ideally, the photoemission intensity measurements should be converted to a partial cross section (I) and the sulfur cross section (I_0) removed. As suggested in Ref. 14, we have adopted a one-step empirical normalization by deriving I_0 as the smooth part of the intensity measurements. This experimental I_0 will contain small contributions from electron-analyzer transmission and low-frequency interferences; we expect errors in the estimated frequency spectra below 1 Å. No reliable estimate of these frequencies is possible even with our 400-eV data range; no useful structure information is lost in this simplified normalization. For S/Ni(100),

$$I_0 = -4.3\times 10^{-5}E^2 + 2.6\times 10^{-2}E + 1.9;$$

for S/Cu(100),

$$I_0 = -5.0\times 10^{-5}E^2 + 3.4\times 10^{-3}E + 1.48.$$

[8]Derived by analogy with P. A. Lee and J. B. Pendry, Phys. Rev. B 11, 2795 (1975). A similar formula from T. Fujikawa [J. Electron Spectrosc. Relat. Phenom. 22, 353 (1981)] differs in sign.

[9]P. Orders and C. Fadley, Phys. Rev. B 27, 781 (1983).

[10]The overlayer was prepared by exposing clean Cu(001) to $\sim 75\times 10^{-6}$ Torr sec H_2S and heating the crystal to ~ 500 K. The $p(2\times 2)$ structure was confirmed by *in situ* low-energy electron diffraction.

[11]S. Brennan, J. Stohr, and R. Jaeger, Phys. Rev. B 24, 4871 (1981).

[12]J. J. Barton and D. A. Shirley, to be published.

[13]P. A. Lee, B. K. Teo, and A. L. Simons, J. Am. Chem. Soc. 99, 3856 (1977).

[14]G. Martens, P. Rabe, N. Schwenter, and A. Werner, Phys. Rev. B 17, 1481 (1978). E_0 was determined empirically by the method of this reference: for S/Ni, $E_0 = 5$ eV; for S/Cu, $E_0 = 11$ eV.

[15]P. A. Lee, Phys. Rev. B 13, 5261 (1976).

[16]B. A. Bunker and E. A. Stern, Phys. Rev. B 27, 1017 (1983).